

## Article

# Investigating the Impact of Aquifer Parameters on Carbon Dioxide Dissolution in Saline Aquifers

Mohsen Abbaszadeh<sup>1\*</sup>, Seyed ShariatiPour<sup>1</sup>

<sup>1</sup> Fluid and Complex Systems Research Center, Coventry University, Priory Street, Coventry CV1 5FB; abbaszam@uni.coventry.ac.uk

\* Correspondence: abbaszam@uni.coventry.ac.uk; Tel.: +447407061712

**Abstract:** CO<sub>2</sub> injection into geological formations is considered one way of mitigating the increasing levels of carbon dioxide concentrations in the atmosphere and its effect on and global warming. In regard to sequestering carbon underground, different countries have conducted projects at commercial scale or pilot scale and some have plans to develop potential formations for carbon dioxide storage. In this study, pure CO<sub>2</sub> injection is examined on a model with the properties of bunter sandstone and then sensitivity analyses were conducted for some of the important parameters. The results of this study show that the extent to which CO<sub>2</sub> has been convected in the porous media in the reservoir plays a vital role in improving the CO<sub>2</sub> dissolution in brine and safety of its long term storage. We conclude that heterogeneity plays a crucial role on the saturation distribution and can increase or decrease the amount of dissolved CO<sub>2</sub> in water. Furthermore, the value of absolute permeability controls the effect of the  $K_v/K_h$  ratio on the CO<sub>2</sub> dissolution in brine. In other words, as the value of vertical and horizontal permeability decreases (i.e. tight reservoirs) the impact of  $K_v/K_h$  ratio on the dissolved CO<sub>2</sub> in brine becomes more prominent. Additionally, reservoir engineering parameters, such as well location, injection rate and scenarios, also have a high impact on the amount of dissolved CO<sub>2</sub>.

**Keywords:** CO<sub>2</sub> Injection, Sensitivity analysis, CO<sub>2</sub> Storage

## 1. Introduction

The global temperature over the last century shows a slight increase and predictions indicate an increase of up to 1.1 – 6.6 °C by the end of this century [1]. Carbon capture and storage (CCS), that comprises of the separation of CO<sub>2</sub> from the gaseous exhaust of power plants and other heavy industries and safe and secure long-term storage in geological formations is considered as the most applicable method for mitigation of CO<sub>2</sub> concentration in the atmosphere [1-3]. Investigations show that there is the potential for nearly 2000 Gt of CO<sub>2</sub> storage capacity within the different underground formations around the world [1]. Different geological formations considered as a sink for CO<sub>2</sub> storage include depleted oil and gas reservoirs, un-mineable coal beds and saline aquifers [4]. Amongst these sites, deep saline aquifers show the highest storage potential [5]. The best storage

sites are those that trap the CO<sub>2</sub> as an immobile phase under the ultra-low permeability confining caprock where it is subject to further gradual physical and chemical trapping mechanisms [1].

The trapping mechanisms active during CO<sub>2</sub> injection into saline aquifers can be described as:

- 1) Hydrodynamic trapping, which is the primary trapping mechanism for CO<sub>2</sub> storage, as a result of capillary pressure of the low permeability caprock [6].
- 2) Residual trapping, which takes place at residual gas saturation where the CO<sub>2</sub> becomes immobile due to the capillary forces and interfacial tension effects [7,2].
- 3) Solubility trapping, where CO<sub>2</sub> dissolves in the formation brine over time during and after injection. The dissolution of CO<sub>2</sub> in water creates carbonic acid that decreases the pH of the environment [8] and;
- 4) Mineral trapping, where the dissolved CO<sub>2</sub> in the form of carbonates and bicarbonates reacts with the minerals of the rock leading to a precipitate as secondary carbonates [9]. Mineral trapping is considered as the safest way of CO<sub>2</sub> storage as it converts to solid precipitation. However this process is very slow.

At the initial stages of injection, the hydrodynamic and structural trapping mechanisms are active [7]. However in the long-term, other trapping mechanisms, such as solubility, residual gas and mineral trapping, will arise.

Nghiem et al. presented a simulation and optimization method for the trapping mechanisms during CO<sub>2</sub> storage in saline aquifers [10]. They adjust the location and the rate of injection to enhance the total amount of CO<sub>2</sub> trapping. Shariatiour et al. proposed an engineering solution for increasing the efficiency of CO<sub>2</sub> dissolution in formation brine [11]. In their method, brine extracted from the top of the aquifer is mixed by a downhole mixing tool with CO<sub>2</sub> which is injected through the tubing. Then, the dissolved CO<sub>2</sub> in brine is injected into the same formation through another lateral at the bottom of the aquifer. The advantage of their concept is that the high pressure of formation water will increase the solubility of CO<sub>2</sub> in water and there is no energy penalty in lifting the brine to the surface for the surface mixing processes. Ide et al. studied the effect of the gravity and viscous forces on residual trapping – also known as capillary trapping – of CO<sub>2</sub> [12]. Their results show that in cases in which the gravitational forces are weaker in comparison with viscous forces, more CO<sub>2</sub> is trapped. Research was conducted by Li et al. to study the effect of capillary pressure on migration behavior of CO<sub>2</sub> plume [13]. Their results show that the capillary pressure has only a minor impact during the injection phase, but will increase during the post-injection processes.

The Bunter sandstone is a reservoir rock which is more than 200 m thick and has a considerable storage potential for CO<sub>2</sub> storage purposes [14, 15, 16]. The Bunter sandstone is comprised of several domes which are mostly saturated with brine while only a few formations are filled with natural gas [17, 18]. Williams et al. created a precise geological model based on the core, seismic and well log data to estimate the storage capacity of domes in Bunter sandstone [16]. They calculated storage efficiencies between 4% (closed domes) to 33% (homogeneous model). Heinmann et al. studied the storage capacity based on a multi-well injection scenario and estimated that 3.8 – 7.8 Gt CO<sub>2</sub> could be stored in the parts of the Bunter sandstone they studied [19]. Our study focuses on the solubility and residual trapping mechanisms and the determination of storage efficiency in a model with the properties of Bunter sandstone closure in the UK sector of the Southern North Sea.

## 2. Model Description

The three dimensional reservoir simulation model for studying CO<sub>2</sub> injection in a saline aquifer was created by the Eclipse 300 through the CO2STORE option. The dimensions of the model are 1600m long, 800m wide and 140m thick. The main input data and the thickness of the formation were adopted from the work by [19]. Table 1 shows the input data used in this study. The  $K_v/K_h$  is assumed to be 0.1 in the base case and since the horizontal permeability is 250 mD, the vertical permeability is 25 mD. Given the lack of relative permeability and capillary pressure data for Bunter sandstone, the data presented by Bennion and Bachu have been used in this study [20].

The injection pressure should not exceed the fracture pressure of the formation rock and the caprock because increasing the pressure more than limit that will create fractures in the rock that will act as pathways for CO<sub>2</sub> leakage to the surface. In this regard, the method presented by Brook et al. was used to calculate the fracture pressure of the formation [21]. We considered the bottom hole pressure constraint as 90% of the fracture pressure of the formation [16]. If the pressure rises beyond this limit the injection well will be shut-in. In all the simulations only one injection well has been presented. In the base case, pure CO<sub>2</sub> is injected at a rate of 1 Mt per year through the tubing to the bottom of the formation for 20 years. Injection then stops and the simulation progresses continue for a further 100 while the flow of fluids is the result of density differences alone. The perforated section is 20 meter high from the bottom of the formation. The static model was considered to be completely saturated with brine and no free gas exists at the beginning of the simulation. Through the use of the Diffusion option, the CO<sub>2</sub> is allowed to dissolve in the formation brine during and after injection. The model presented by Spycher and Pruess was used to calculate the CO<sub>2</sub> dissolution in brine [8]. They studied the behavior of a mixture of H<sub>2</sub>O-CO<sub>2</sub> at the temperatures between 12 – 100 °C and pressures up to 600 bar. It is well-known that the solubility of CO<sub>2</sub> in water increases with pressure and decreases with an increase in temperature and salinity. In contrast, in deeper aquifers both temperature and the salinity increase and thus the dissolution of CO<sub>2</sub> in formation brine decreases. However, it should be noted that aquifers with greater depth are considered to be interesting sinks for CO<sub>2</sub> storage because they are safer and the geothermal energy can be also utilized alongside the CCS [22, 23, 24].

Table 1: Input data for the basic model

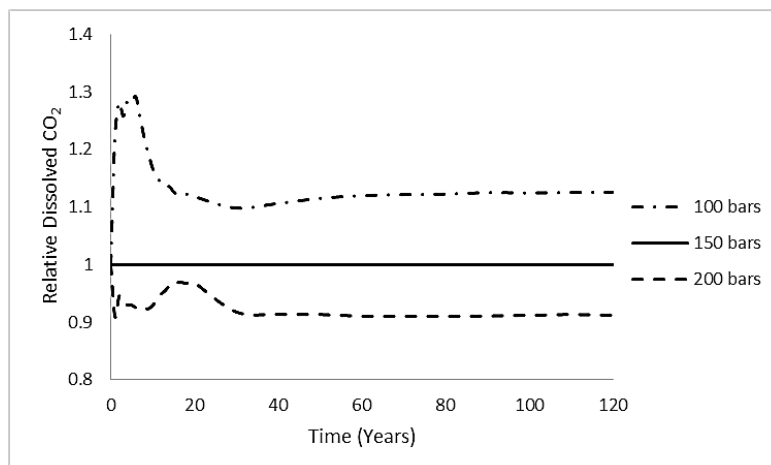
| Input Data           | Value        | Units   |
|----------------------|--------------|---------|
| H. Permeability      | 250          | mD      |
| V. Permeability      | 25           | mD      |
| Porosity             | 0.18         | -       |
| Depth                | 1500         | m       |
| Number of Blocks     | 80 * 40 * 70 | -       |
| Blocks Dimensions    | 20 * 20 * 2  | m       |
| Rock Compressibility | 5.56*E-5     | 1/bars  |
| Temperature          | 55           | °C      |
| Pressure             | 150          | bars    |
| Thickness            | 140          | m       |
| Injection Rate       | 1            | Mt/year |

One of the main objectives of this study is to determine the CO<sub>2</sub> storage efficiency that is known to be dependent on different factors which can be categorised as: 1) Characteristics of the target aquifer for storage such as porosity, permeability, temperature, pressure, etc; 2) Characteristics of CO<sub>2</sub> storage operation such as injection rate, number of wells, etc; 3) Constraints used in the injection process, such as maximum bottom hole pressure and the definitions used to calculate the volume of rock which is considered for CO<sub>2</sub> storage [25]. Different researchers have proposed different methods for the estimating CO<sub>2</sub> efficiency. A task force of the Carbon Sequestration Leadership Forum has presented methods for calculating storage efficiency in hydrocarbon reservoirs, coal beds and saline aquifers [7]. In another work, the US Department of Energy has developed a method for estimating CO<sub>2</sub> storage capacity in the mentioned media [26]. Considering the limitations for pressure build up in the model, the storage efficiency is calculated by the formula used by Williams et al. [13]. The volume of CO<sub>2</sub> injected is calculated by the dynamic simulation.

### 3. Results and Discussion

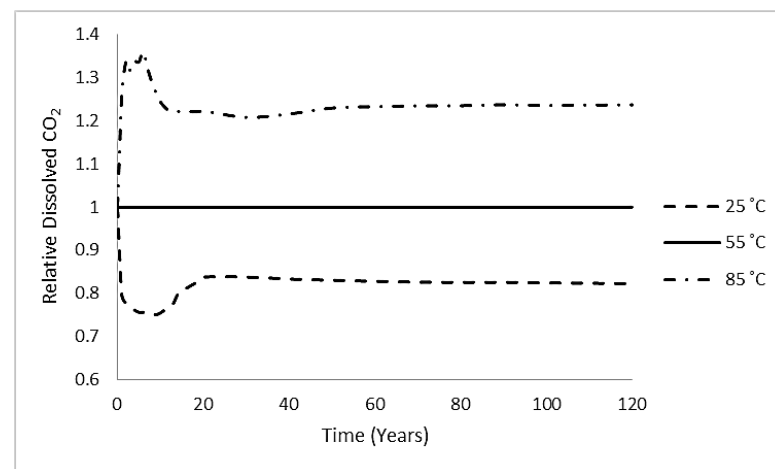
In order to define the effect of different parameters on the CO<sub>2</sub> storage in the Bunter sandstone, some sensitivity analysis were conducted on the model. To obtain the impact of one parameter, the simulation is run by changing the value of that parameter while all other parameters are kept constant. Understanding the change of several parameters at the same time will be considered in future studies. It should be noted that here we investigate the impact of each parameter on the amount of dissolved CO<sub>2</sub> in the brine.

Fig. 1 shows the sensitivity analysis on initial pressure of the aquifer. Two different pressures (100 bars and 200 bars) were considered other than the pressure of the basic model. As can be seen in Fig. 1 the amount of dissolved CO<sub>2</sub> has decreased with an increase in reservoir pressure; which might seem in contradiction with our former expectation that the solubility of CO<sub>2</sub> increases with increase in pressure. This can be attributed to the increase in reservoir pressure that increases the density and viscosity of CO<sub>2</sub> that results in a decrease in the mobility of CO<sub>2</sub>. Thus, the distribution of CO<sub>2</sub> in the porous media becomes less and it come into less contact with the fresh brine. This result is in agreement with the former result in the literature [27]. The storage efficiencies from the lowest pressure to the highest are, 3.4 %, 2.6% and 2.3%, respectively.



**Fig. 1:** Effect of pressure (bar) on CO<sub>2</sub> dissolution in brine vs time.

The effect of initial aquifer temperature is presented in Fig. 2. As it is shown the dissolution of CO<sub>2</sub> in brine increases with temperature, which again contradicts the well-known principle that the solubility of CO<sub>2</sub> decreases with increased temperature. This observed increased dissolution is due to the increase in mobility of CO<sub>2</sub> and far easier movement through the medium and contact with fresh brine. This is in agreement with results of previous research by Kumar et al. [27, 28]. The storage efficiencies are calculated as 2%, 2.6% and 3.7 % for the lowest to the highest temperature, respectively.



**Fig. 2:** Effect of temperature (°C) on CO<sub>2</sub> dissolution in brine vs time.

The effect of IFT is presented in Fig. 3. IFT is a parameter which has a great impact on the relative permeability and capillary pressure curves, distribution of fluids in porous media and miscibility of them. To see the impact of IFT on dissolution of CO<sub>2</sub> in brine three different relative permeability and capillary pressure curves corresponding to three different IFT values have been input to the model from [20]. The results show that as the IFT decreases the dissolution of CO<sub>2</sub> in brine increases.

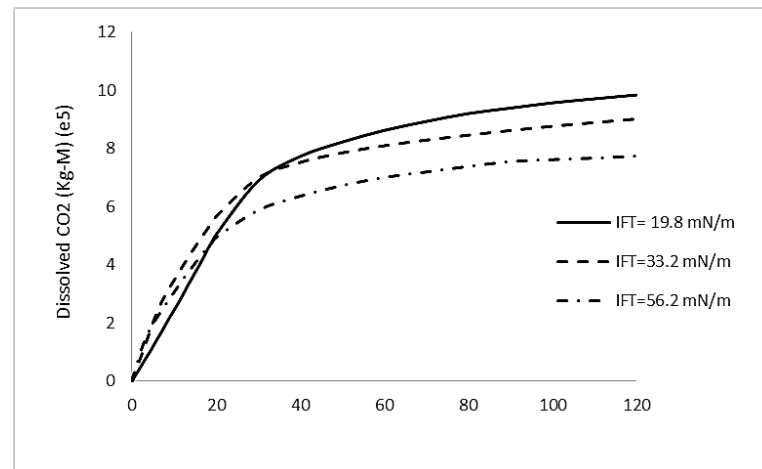


**Fig. 3:** Effect of IFT on CO<sub>2</sub> dissolution in brine vs. time.

The effect of different injection rates are presented in Fig. 4. This figure shows that the dissolution of CO<sub>2</sub> in brine has a direct relationship with the injection rate. As the injection rate increases the amount of CO<sub>2</sub> in contact with brine and the distribution also increase, thus the dissolution rate increases. Moreover, as can be seen in Fig. 4, the possibility of CO<sub>2</sub> plumes becoming isolated and

remaining as residual gas increases with the increase in the injection rate; because the distribution of CO<sub>2</sub> in the medium increases. Based on the simulations, the storage efficiencies for the lowest to the highest injection rate are 0.5%, 2.6% and 5%, respectively. However, it should be noted that for the lowest injection rate (one fifth of the base case), 24.11% of the total amount of injected CO<sub>2</sub> is dissolved while in the base model and the higher injection rate (two times of the base case) only 17.21% and 14.21% of the total injected gas is dissolved, respectively. In the other words, the percentage of dissolved CO<sub>2</sub> in the lower injection rate is higher than the amount of dissolved CO<sub>2</sub> in the higher injection rate.

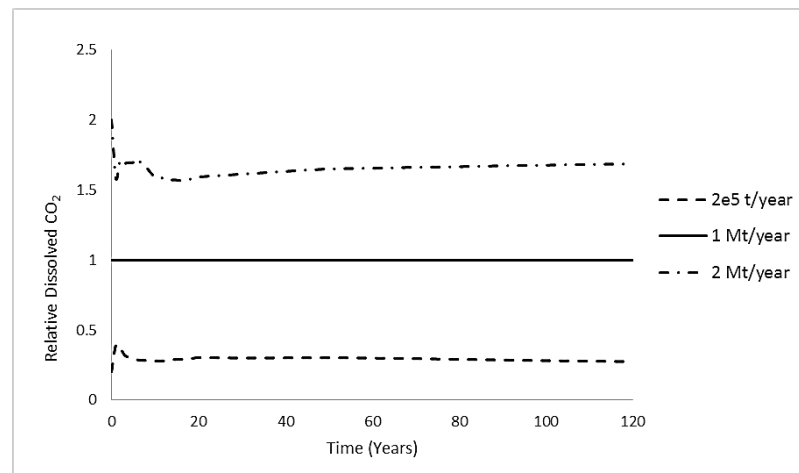


**Fig. 4:** Effect of injection rate on CO<sub>2</sub> dissolution in brine vs time.

Fig. 5 shows a comparison between the impacts of temperature, pressure and injection rate. As can be seen, injection rate has the highest impact and pressure and temperature have nearly close and less impact on CO<sub>2</sub> dissolution in brine.

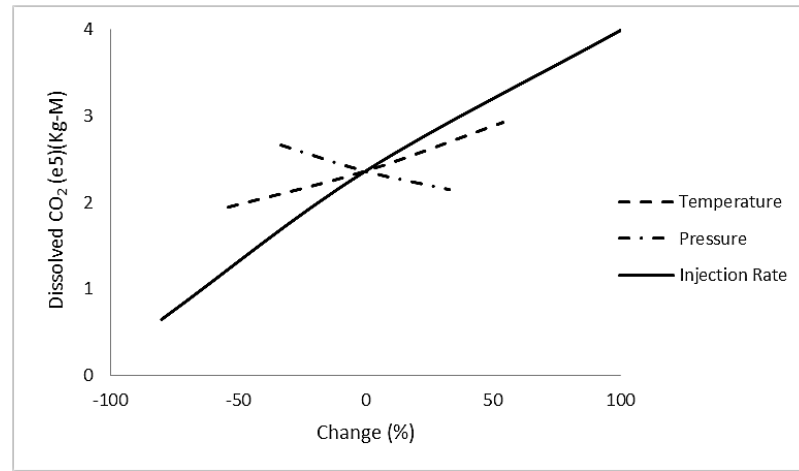


**Fig. 5:** Comparison between the impact of Temperature, Pressure and Injection Rate.

At this stage, we considered one injection scenario and compare the results of it with the base case. In this scenario, the CO<sub>2</sub> is injected to the system for five years and then the injection stops for next five years. This interval continues for other three times until we have a total of 20 years of injection. Following the final five-year shut-in the simulation runs a further 85 years. This scenario can be applicable to the condition where we don't have a continuous access to the CO<sub>2</sub> source. On the other hand since the dissolution of CO<sub>2</sub> in brine is a very slow process, the appropriate time is given to this

process after each shut-in, while at the same time the pressure of the reservoir stays low resulting in the ability to inject higher amounts of CO<sub>2</sub> over longer time intervals. It should be noted that all the other parameters in the simulations remain constant in both scenarios. Results show the amount of dissolved CO<sub>2</sub> in brine in this case is 5.5% higher than in the base case at the end of the injection period, although it happens in 15 years later (Fig 6). After the injection stops at late post-injection times the amount of dissolved CO<sub>2</sub> proceeds towards a same plateau for both cases. It can be concluded from these two scenarios that Case 1 shows a reasonable performance in a situation where we do not have a continuous access to CO<sub>2</sub> source. The storage efficiencies are 2.6% for both injection scenarios based on Equation presented by William et al. [16].

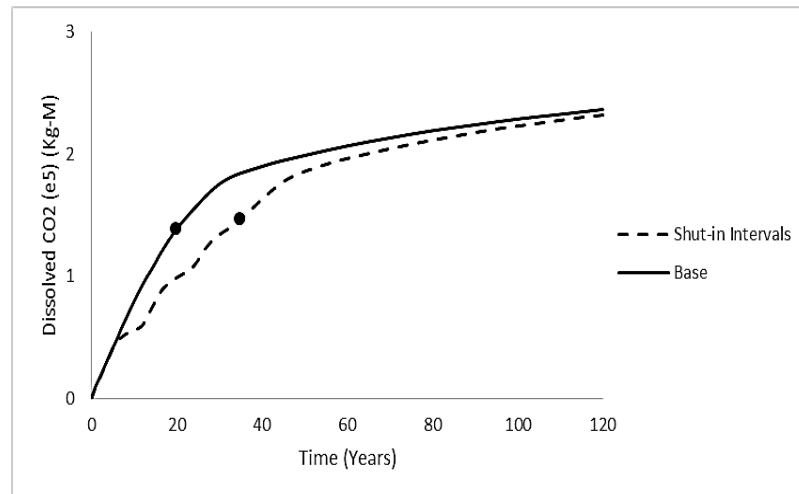


**Fig. 6:** Effect of injection period on CO<sub>2</sub> dissolution in brine vs time.

In this stage we investigate the effect of vertical to horizontal permeability in our study. In order to investigate the effect of vertical to horizontal permeability, first, we changed the value of vertical permeability to create different ratios and the results we achieved are different from the former approach. As can be seen in Fig. 7, the amount of dissolved CO<sub>2</sub> in brine is the highest for the ratio of 0.1 before and after shut-in. However, the amount of dissolved CO<sub>2</sub> in brine for 0.01 is lower than the ratio of 1 before the injection stops and then increases after shut-in. Since the results we achieved are not in agreement with the results by former researchers for pre-shut-in duration [24], the effect of vertical to horizontal permeability on the amount of dissolved CO<sub>2</sub> with different absolute permeability values is investigated.

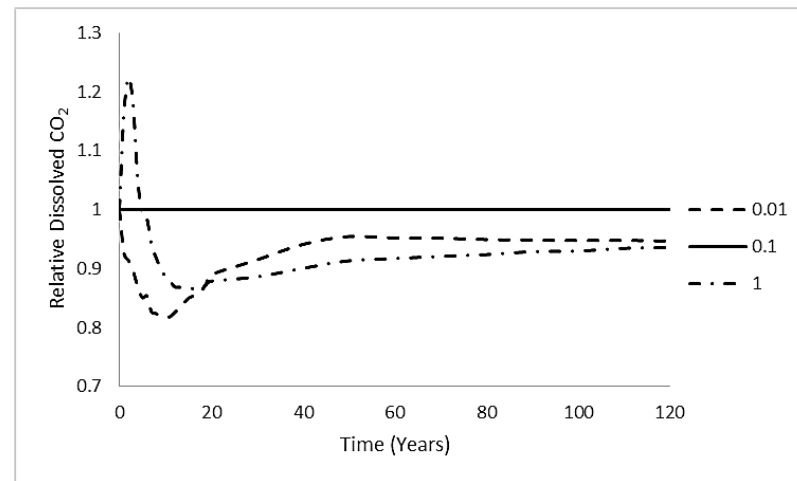


**Fig. 7:** Effect of  $K_v/K_h$  ratio on the amount of dissolved  $\text{CO}_2$  vs time by changing  $K_v$ . In another approach, we change the value of horizontal permeability to achieve different ratios of vertical to horizontal permeability. Results show the amount of dissolved  $\text{CO}_2$  in the brine has increased as the vertical to horizontal permeability has decreased (Fig. 8). This is because of the easier distribution of  $\text{CO}_2$  in the reservoir through the increase in horizontal permeability. The simulations show that the storage efficiency is 2.6% for all cases. This results show that although that the storage efficiencies are the same, the higher the  $K_h$  is, the more the reservoir is suitable for storage purposes by an increase in dissolved  $\text{CO}_2$ .

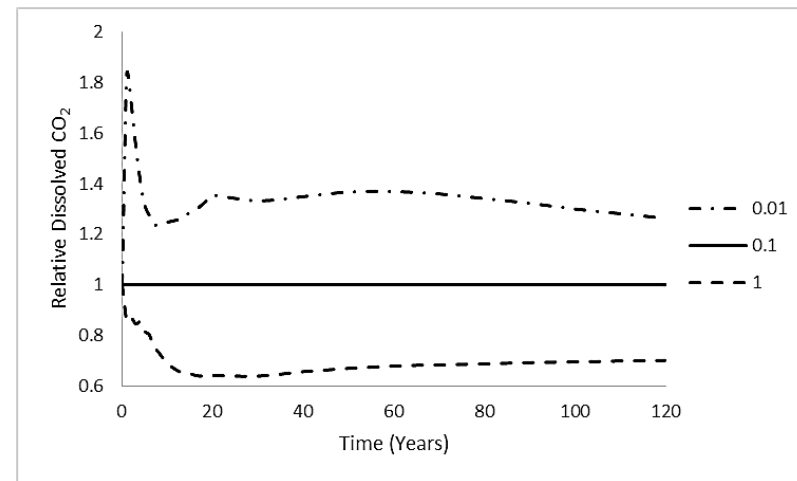


**Fig. 8:** Effect of  $K_v/K_h$  ratio on  $\text{CO}_2$  dissolution in brine vs time by changing  $K_h$ .

As presented in Fig. 9, the curve for the amount of dissolved  $\text{CO}_2$  in brine for  $K_v/K_h$  ratio of 0.01 shows a decreasing trend from the high permeability pairs to low permeability pairs and at the lowest value of absolute permeabilities it shows the least amount of dissolved  $\text{CO}_2$  either before and after shut-in. This is because when the value of absolute permeabilities decreases the effect of  $K_v/K_h$  ratio of 0.01 becomes more acute, since the  $\text{CO}_2$  plume propagation in the vertical direction decreases abruptly and the movement and contact of  $\text{CO}_2$  with water intensively decreases. On the other hand, from the plots in Fig. 9 it can be concluded that as the value of vertical and horizontal permeability decreases (for instance in tight reservoirs) the impact of the  $K_v/K_h$  ratio on the amount of dissolved  $\text{CO}_2$  increases, as shown by the increasing space between the curves in each plot. While it should be noted that more  $\text{CO}_2$  is dissolved by the ratio of 0.1 in all cases.

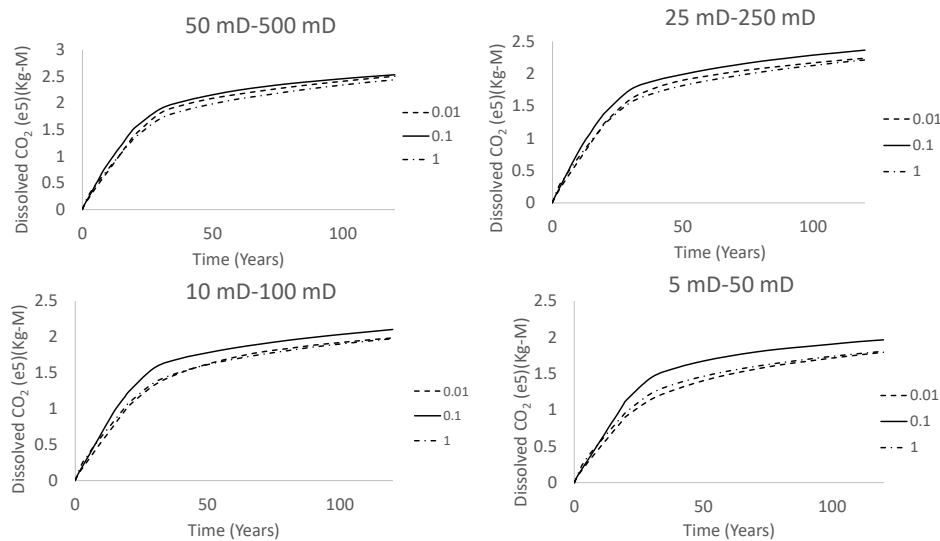


**Fig. 9:** Control of absolute permeability on  $K_v/K_h$  ratio on  $\text{CO}_2$  dissolution in brine (by changing  $K_v$ ).

Then, some sensitivity analysis is performed on the impact of number of cell connections of the wellbore and the reservoir. The connections are considered from cell No. 15 to 70 to the cell No. 69 to 70 in the vertical direction. As Fig. 10 demonstrates the connections with the highest numbers of cells (i.e. 15-70 and 30-70) does not have the highest dissolution of  $\text{CO}_2$  in brine. Because with the high number of cell connections  $\text{CO}_2$  will move upwards quickly and creates a plume under the top of the reservoir; therefore, does not have enough time to be in contact with fresh brine and the dissolution decreases. Thus, there is a maximum number of cell connections that creates the highest dissolution value and the dissolution decreases for higher numbers of cells.

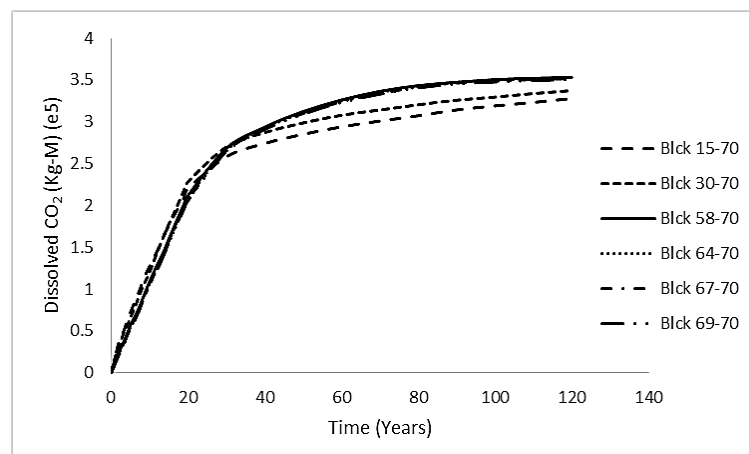


**Fig. 10:** Effect of the number of cell connections between well and reservoir.

In order to investigate the impact of permeability heterogeneity, a model with the same geometry was developed, with the permeability being changed while maintaining the same mean with the homogeneous model. As is exhibited in Fig. 11, by imposing the heterogeneity the amount of dissolved  $\text{CO}_2$  decreased during the injection period compared with the homogeneous model and then increased after the injection stops. This is because during the injection period in the homogeneous model the  $\text{CO}_2$  plume proceeds easier in the porous media and is in contact with more fresh brine, thus the dissolution rate is higher. After the injection stops, since the  $\text{CO}_2$  plume has a

non-uniform distribution in heterogeneous model, the surface area of  $\text{CO}_2$  plume in contact with brine is higher than the homogeneous model and dissolution increases. In addition, in the heterogeneous model, due to the slower movement of  $\text{CO}_2$  plume, there is enough time for dissolution trapping. In the homogeneous model the  $\text{CO}_2$  model very soon accumulates in the top of the formation and its contact with the formation brine decreases. The storage efficiency is 2.6% for both homogeneous and heterogeneous systems.

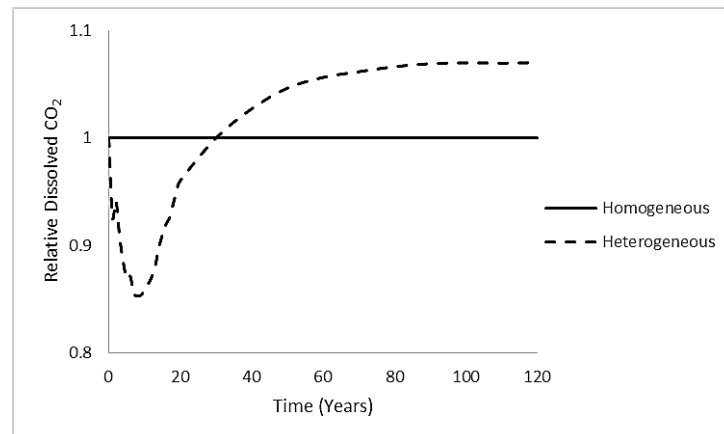


**Fig. 11:** Effect of heterogeneity on  $\text{CO}_2$  dissolution in brine vs time.

At this stage the impact of different cases of heterogeneity is investigated. Thus, different series of permeability heterogeneity data was generated in order to determine what the effect of different heterogeneity data will be on the model. Thus, at this stage 20 different permeability heterogeneity data were generated having the same mean permeability as the homogeneous permeability (250 mD horizontal permeability and 25 mD vertical permeability). Since the amount of data is huge we only present 10 of the data for  $\text{CO}_2$  dissolution in brine at the end of the injection and at the end of the simulation (after 120 years). As can be seen in Fig. 12, the amount of dissolved  $\text{CO}_2$  in brine varies significantly based on the permeability heterogeneity data and does not obey a rational rule, being either greater or less than the homogeneous model. The only result which is in agreement with the results from the first sensitivity analysis conducted on heterogeneity is that the amount of dissolved  $\text{CO}_2$  in the homogeneous model is less than that of all the heterogeneous models in the long term. It should be noted that in all these cases the range that the horizontal permeabilities are generated is between 5 mD to 600 mD and the standard deviation is 200, while the range of vertical permeability is between 0.5 mD to 55 mD and the standard deviation is 20. All the percentages are in comparison to the homogeneous model.

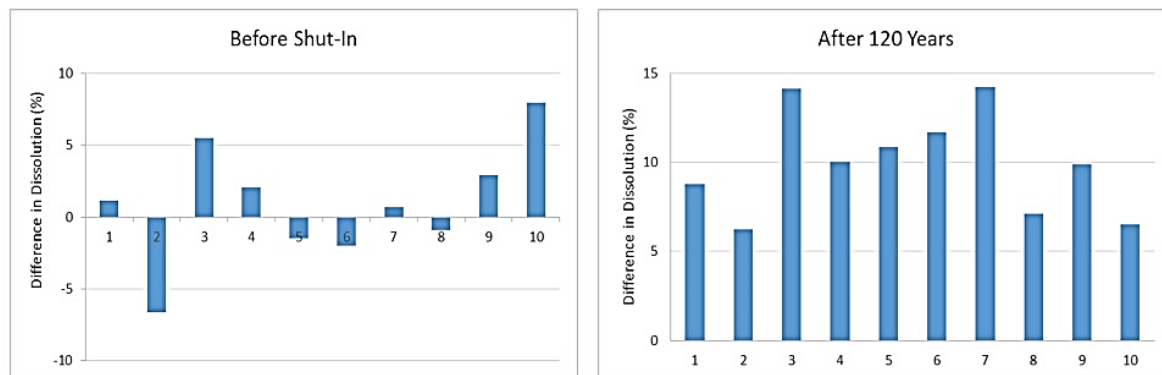


Fig. 12: Increase/decrease in permeability for different permeability heterogeneity data.

The variation in the amount of dissolved CO<sub>2</sub> in brine in the heterogeneous cases is due to the different saturation distribution of the gas phase in the porous medium which creates different contact areas between the brine and CO<sub>2</sub>. As presented in Fig. 12, while the mean permeability remains the same in all cases, the saturation distribution varies considerably from case to case. Here only 6 cases are shown.

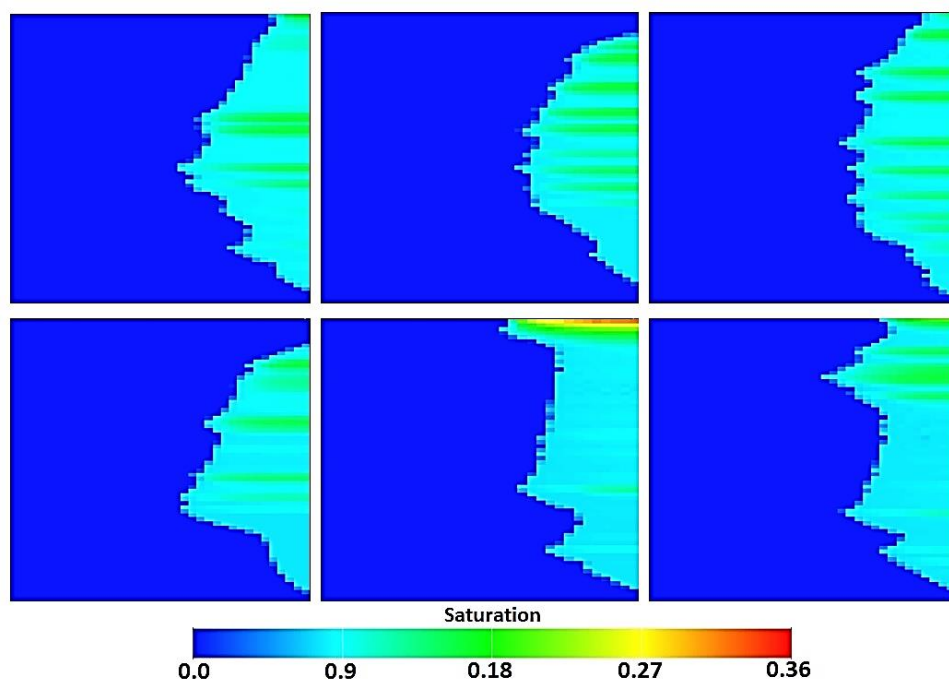


Fig. 12: Gas saturation distribution after 120 years in 6 different cases.

In order to investigate the effect of the range in which the permeability data are generated we first only changed the maximum of the ranges while all the other parameters are kept constant. In another sequence we tested different minimum and maximum values for the range in which the permeability data is supposed to be generated. In all these cases no rational trend was observed and the dissolution data is seen to be different in each case. The data for each case is presented in Table 3 and Table 4, respectively.

Table 3: data of increase/decrease of CO<sub>2</sub> dissolution in brine with changing the maximum of the range.

| Case No.                                  | After Shut-in (20 Years)<br>(%) | After 120 Years<br>(%) |
|---|---------------------------------|------------------------|
| 11 (0.5 mD to 40 mD) & (5 mD to 500)      | -1.60                           | 11.36                  |
| 12 (0.5 mD to 70 mD) & (5 mD to 900 mD)   | -0.92                           | 10.79                  |
| 13 (0.5 mD to 100 mD) & (5 mD to 1100 mD) | 4.88                            | 12.10                  |
| 14 (0.5 mD to 150 mD) & (5 mD to 1400 mD) | -0.43                           | 8.06                   |

Table 4: Data of increase/decrease of CO<sub>2</sub> dissolution in brine for different ranges.

| Case No.                                 | After Shut-in (20 Years)<br>(%) | After 120 Years<br>(%) |
|--|---------------------------------|------------------------|
| 15 (5 mD to 40 mD) & (100 mD to 450 mD)  | 0.82                            | 2.33                   |
| 16 (15 mD to 70 mD) & (25 mD to 650 mD)  | 1.97                            | 2.74                   |
| 17 (20 mD to 30 mD) & (150 mD to 500 mD) | 3.63                            | 1.10                   |
| 18 (1 mD to 90 mD) & (200 mD to 800 mD)  | 6.37                            | 5.42                   |
| 19 (10 mD to 80 mD) & (50 mD to 800 mD)  | 0.56                            | -0.61                  |

In another approach, we change the value of the standard deviation while keeping the minimum and maximum of the range constant. In this approach we find that in Cases 20 and 21 when that the standard deviation is low the values are closer to the mean (which is 25 mD and 250 mD) but are still random values as in the first 10 cases. Thus, there is no rational trend in the amount of dissolved CO<sub>2</sub> in brine. However, as the standard deviation increases (more than 30), the random numbers generated are getting closer to the value of minimums and maximums and the amount of dissolved CO<sub>2</sub> in brine decreases. This observation is attributed to the phenomenon that the very small values of permeability does not enable the CO<sub>2</sub> phase to distribute within the porous medium and is therefore not in contact with the brine. Thus, the dissolution of CO<sub>2</sub> in brine decreases (Table 5).

Table 5: Data of increase/decrease of CO<sub>2</sub> dissolution in brine with changing standard deviation.

| Case No.          | After Shut-in (20 Years)<br>(%) | After 120 Years<br>(%) |
|-------------------|---------------------------------|------------------------|
| 20 (S.D.= 5&50)   | 1.28                            | 0.58                   |
| 21 (S.D.= 10&100) | 3.81                            | 1.12                   |
| 22 (S.D.= 30&300) | 0.20                            | 4.98                   |
| 23 (S.D.= 40&400) | -4.59                           | 3.29                   |
| 24 (S.D.= 80&700) | -4.60                           | 2.24                   |

|                     |        |       |
|---------------------|--------|-------|
| 25 (S.D.= 100&900)  | -8.66  | -1.27 |
| 26 (S.D.= 200&1100) | -10.03 | -4.33 |

It is worth mentioning that in considering the maximum and minimum value of the amount of dissolved CO<sub>2</sub> in brine for 36 different permeability heterogeneity cases with the same mean the following observation identified. We observed that the maximum value of dissolved CO<sub>2</sub> at the time of shut-in is 39.2% more than the minimum value and the maximum value 100 years after shut-in is 19.41% more than the minimum. This considerable difference in the solubility proves the importance of permeability heterogeneity in the amount of dissolved CO<sub>2</sub> and the saturation distribution which must be created based on the precise and real data of the target formation for CO<sub>2</sub> storage.

In another attempt to cover the different aspects of permeability heterogeneity we changed the well location while the same permeability data is used in the model. In this regard, we considered four different well locations in the model. The results show that even by changing the well location in the same model the amount of dissolved CO<sub>2</sub> is changed (Table 6).

Table 6: Difference in CO<sub>2</sub> dissolution by changing well location compared to the base case.

| Case No.                     | After Shut-in (20 Years)<br>(%) | After 120 Years<br>(%) |
|------------------------------|---------------------------------|------------------------|
| 1 (Symmetry to the base)     | -1.21                           | -1.66                  |
| 2 (Centre of the model)      | 23.75                           | 11.52                  |
| 3 (blocks 20&10 in XY plane) | 26.71                           | 13.51                  |
| 4 (Blocks 60&30 in XY plane) | 25.43                           | 11.60                  |

Since in the base case the well is located in a corner of the model, the abrupt increase observed in the well locations other than the corners (Cases 2, 3 and 4) is due to the lack of boundary effects which decrease wellbore contact with fresh brine. Although, the difference is still sensible between the symmetry cases.

Now the impact of horizontal well is investigated in the CO<sub>2</sub> dissolution in brine. In this regard, CO<sub>2</sub> is injected through a horizontal well with the same number of connection cells to the reservoir. The saturation distribution is shown in Fig. 12.

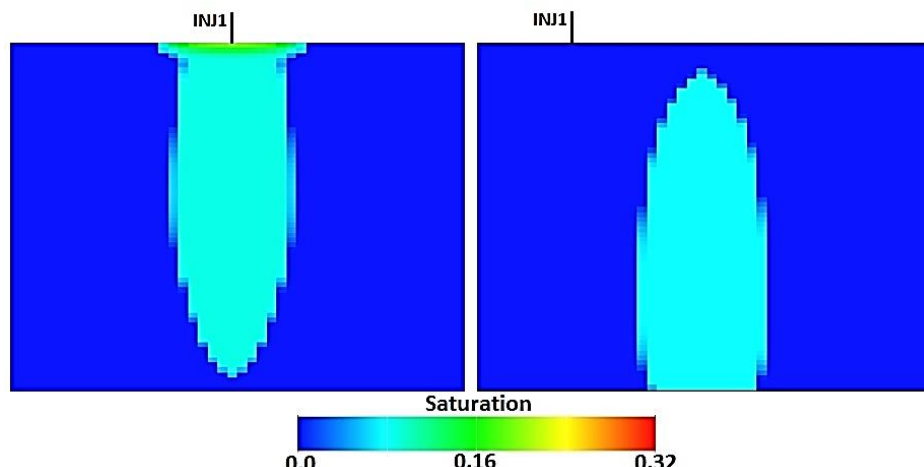


Fig. 12: Gas saturation distribution by vertical (left) and horizontal well (right).

To compare the impact of vertical and horizontal wells, first  $\text{CO}_2$  is injected through a vertical well completed from grid No. 60 to grid No. 70 which creates a 20 meter perforation section. On the other hand, since the grid size in the X direction is 20 meters first  $\text{CO}_2$  is injected through only one grid in the X direction. Then by the use of Local Grid Refinement (LGR) option one grid in the X direction is refined to 10 grids which are 2 meters each and all ten grids are allowed to flow. The simulation results presented in Fig. 13 shows that injecting  $\text{CO}_2$  with the same rate by horizontal and vertical wells does not make a considerable difference in the amount of dissolved  $\text{CO}_2$  in brine in a homogeneous system.

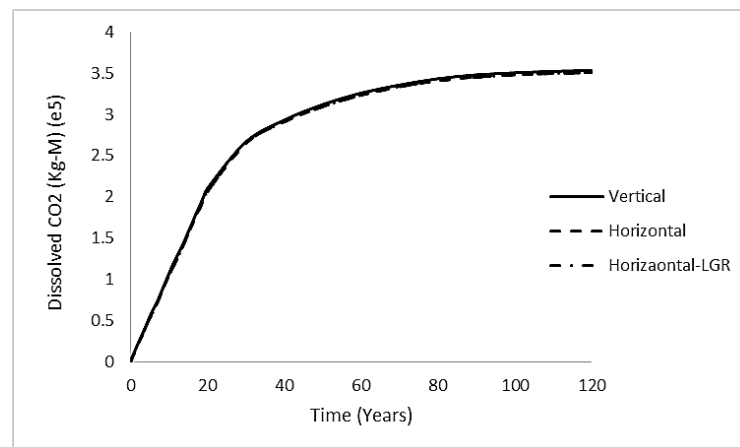


Fig. 13: Effect of vertical and horizontal wells on  $\text{CO}_2$  dissolution in brine.

We further expanded our study to investigate the effect of different heterogeneity distribution in the reservoir by dividing the reservoir into two layers by imposing two different sets of permeability heterogeneity data created by a high and a low standard deviation. In our first case the permeability heterogeneity data that has been created by higher standard deviation was located in the upper layer. We conducted this simulation using two different sets of heterogeneity data (Cases A and B). The results show that in the both sets of permeability heterogeneity data when the layer with the higher standard deviation is located down the amount of dissolved  $\text{CO}_2$  in the water is higher (Fig. 12). A slower upward movement of the  $\text{CO}_2$  plume is due to the reason explained in the section investigating the effect of standard deviation and appropriate time to stay in contact with brine is considered as the reason for this observation.

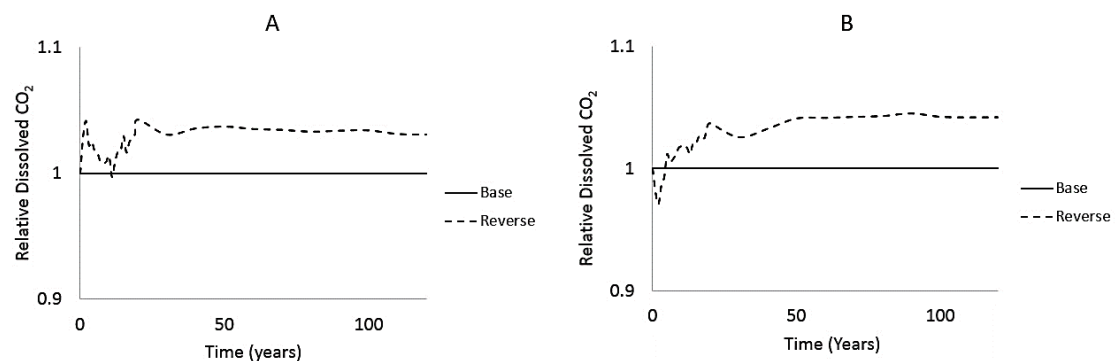


Fig. 13: Effect of two layers of permeability heterogeneity on the dissolution of  $\text{CO}_2$  in brine in two cases.

## 5. Conclusions

In this study we presented a model to predict the consequences of the injection of pure CO<sub>2</sub> in the Bunter sandstone and conducted some sensitivity analysis on different reservoir and injection parameters. In general, the results from this study show that:

- When CO<sub>2</sub> is injected with a same rate in a reservoir with a lower pressure, the amount of CO<sub>2</sub> dissolved and in general, the storage efficiency is higher. In other words, in developing a field for CO<sub>2</sub> storage, injecting CO<sub>2</sub> to the part of the field which has a lower pressure will increase the storage efficiency of the project in addition to operational advantages of working with lower pressures.
- Based on the results of this simulation, when the thermodynamic conditions of the reservoir remains constant, the value of the storage efficiency remains constant. However, to what extent a reservoir is suitable for storage purposes and can efficiently store CO<sub>2</sub> also depends on other factors such as heterogeneity,  $K_v/K_h$  ratio, injection rate, etc. Thus, this equation must be revised and the effect of these parameters must be included in storage efficiency calculation. This will be investigated in the future work.
- One of the most important concepts in evaluating the efficiency and safety of storage is how the CO<sub>2</sub> plume is distributed within the reservoir. In other words, we should consider how much and how easily CO<sub>2</sub> can be distributed within the reservoir when deciding on developing a field and the subsequent location of wells in the reservoir.
- The results of our study show that the vertical to horizontal permeability ratio has a significant impact on CO<sub>2</sub> storage efficiency and the value of absolute vertical and horizontal permeability controls the impact of  $K_v/K_h$  ratio on the dissolution of CO<sub>2</sub> in brine. Furthermore, in low permeability reservoirs the effect of vertical to horizontal permeability on the dissolution of CO<sub>2</sub> in water is more sensible than in the high permeability reservoirs.
- Heterogeneity plays an important role in aquifer performance and the amount of dissolved CO<sub>2</sub> in brine. The results of our study show that different heterogeneity data can result in different amounts of CO<sub>2</sub> being dissolved in brine which might be lower or higher than the homogeneous model. In this regard, the reservoir performance cannot be judged by just adding one set of heterogeneity data. Applying precise and correct heterogeneity data is crucial when investigating the dissolution by simulations. Higher standard deviation in producing heterogeneity data with the same mean will result in decrease in solubility of CO<sub>2</sub> in brine.

**Acknowledgments:** The authors of this study wish to thank Schlumberger for the use of ECLIPSE 300 and Petrel and Amarile for the use of the RE-Studio. Additionally, the contribution of Dr. Philip Costen in this work is highly acknowledged.

## References

1. Metz, B., Davidson, O., De Coninck, H., Loos M., Meyer L.: IPCC special report on carbon dioxide capture and storage, Intergovernmental Panel on Climate Change, Geneva (Switzerland), (2005). Working Group III
2. Bachu, S.: CO<sub>2</sub> storage in geological media: role, means, status and barriers to deployment. *Prog. Energy Combust. Sci.* (2008) 34(2), 254-273.

3. Jiang, X.: A review of physical modelling and numerical simulation of long-term geological storage of CO<sub>2</sub>. *Appl. Energ.* (2011) 88(11), 3557-356.
4. Juanes, R., Spiteri, E., Orr, E., Blunt, M.: Impact of relative permeability hysteresis on geological CO<sub>2</sub> storage. *Water Resour. Res.* (2006) 42(12)
5. Garcia, S., Kaminska, S., Maroto-Valer, M., Underground carbon dioxide storage in saline formations. *Proceedings of the Institution of Civil Engineers-Waste and Resource Management*, (2010) Thomas Telford Ltd.
6. Chiquet, P., Daridon, J.-L., Broseta D., and Thibeau S.: CO<sub>2</sub>/water interfacial tensions under pressure and temperature conditions of CO<sub>2</sub> geological storage. *Energ. Convers Manage.* (2007) 48(3), 736-744
7. Bachu, S., Bonijoly, D., Bradshaw, J., Burruss, R., Holloway, S., Christensen N. P., Mathiassen O. M.:CO<sub>2</sub> storage capacity estimation: methodology and gaps. *Int. J. Greenhouse Gas Control.* (2007) 1(4), 430-443
8. Spycher, N., Pruess, K., CO<sub>2</sub>-H<sub>2</sub>O mixtures in the geological sequestration of CO<sub>2</sub>. Partitioning in chloride brines at 12–100 °C and up to 600 bar. *Geochim. Cosmochim. Ac.* (2005) 69(13), 3309-3320.
9. Xu, T., Apps, J. A., Pruess K., Yamamoto H., Numerical modeling of injection and mineral trapping of CO<sub>2</sub> with H<sub>2</sub>S and SO<sub>2</sub> in a sandstone formation. *Chem. Geol.* (2007) 242(3), 319-346.
10. Nghiem, L., Shrivastava, V., Kohse, B., Hassam M., Yang C., Simulation and optimization of trapping processes for CO<sub>2</sub> storage in saline aquifers. *J. Can. Petrol. Technol.* (2010) 49(08), 15-22.
11. Shariatipour, S. M., Mackay, E. J., Pickup, G. E.: An engineering solution for CO<sub>2</sub> injection in saline aquifers. *Int. J. Greenhouse Gas Control.* (2016) 53, 98-105.
12. Ide, S. T., Jessen, K., Orr F. M.: Storage of CO<sub>2</sub> in saline aquifers: Effects of gravity, viscous, and capillary forces on amount and timing of trapping. *Int. J. Greenhouse Gas Control.* (2007) 1(4), 481-491
13. Li, D., He, Y., Zhang, H., Xu, W., Jiang, X.: A numerical study of the impurity effects on CO<sub>2</sub> geological storage in layered formation. *Appl. Energ.* (2017) 199, 107-120
14. Holloway, S., Vincent, C. J., Bentham M. S., Kirk K. L.: Top-down and bottom-up estimates of CO<sub>2</sub> storage capacity in the United Kingdom sector of the southern North Sea basin. *Environ. Geosci.* (2006) 13(2), 71-84.
15. Noy, D., Holloway, S., Chadwick, R. , Williams, J. , Hannis S., Lahann R.: Modelling large-scale carbon dioxide injection into the Bunter Sandstone in the UK Southern North Sea. *Int. J. Greenhouse Gas Control.* (2012) 9, 220-233.
16. Williams, J., Jin, M., Bentham, M., Pickup, G., Hannis S., Mackay E.: Modelling carbon dioxide storage within closed structures in the UK Bunter Sandstone Formation. *Int. J. Greenhouse Gas Control.* (2013) 18: 38-50.
17. Cameron, T., Crosby, A., Balson, P., Jeffery, D., Lott, G., Bulat J., Harrison D.: The geology of the southern North Sea. United Kingdom, (1992), United Kingdom offshore regional report, British Geological Survey
18. Bentham, M.: An assessment of carbon sequestration potential in the UK–Southern North Sea case study. (2006) Nottingham: Tyndall Centre for Climate Change Research,
19. Heinemann, N., Wilkinson, M., Pickup, G. E., Haszeldine R. S., Cutler N. A.: CO<sub>2</sub> storage in the offshore UK Bunter sandstone formation. *Int. J. Greenhouse Gas Control.* (2012) 6, 210-219
20. Bennion, B., Bachu, S.: Drainage and imbibition relative permeability relationships for supercritical CO<sub>2</sub>/brine and H<sub>2</sub>S/brine systems in intergranular sandstone, carbonate, shale, and anhydrite rocks. *SPE Reservoir Evaluation & Engineering* (2008) 11(03), 487-496
21. Brook, M., Shaw, K., Vincent C., Holloway, S.: Gestco case study 2a-1: storage potential of the bunter sandstone in the UK sector of the southern North Sea and the adjacent onshore area of Eastern England. (2003)
22. Salimi, H., Wolf K. H.: Integration of heat-energy recovery and carbon sequestration. *Int. J. Greenhouse Gas Control.* (2012) 6, 56-68.

23. Ganjdanesh, R., Bryant, S., Orbach, R., Pope G., Sepehrnoori K.: Coupled carbon dioxide sequestration and energy production from geopressured/geothermal aquifers. *SPE J.* (2014) 19(02): 239-248
24. Shariati, S. M., Pickup, G. E., Mackay E. J., Simulations of CO<sub>2</sub> storage in aquifer models with top surface morphology and transition zones. *Int. J. Greenhouse Gas Control.* (2016) 54, 117-128.
25. Bachu, S.: Review of CO<sub>2</sub> storage efficiency in deep saline aquifers. *Int. J. Greenhouse Gas Control.* (2015), 40, 188-202
26. NETL, M., Carbon Sequestration Atlas of the United States and Canada. 1st ed. The U.S. Department of Energy, Office of Fossil energy, (2007).
27. Sifuentes, W., Blunt, M., J., Giddins, M., A., Modeling CO<sub>2</sub> Storage in Aquifers: Assessing the key contributors to uncertainty, SPE Offshore Europe Oil and Gas Conference and Exhibition, Aberdeen, UK, (2009), SPE 123582
28. Kumar, A., Noh, M. H., Ozah, R. C., Pope, G. A., Bryant, S. L., Sepehrnoori, K., Lake, L. W.: Reservoir simulation of CO<sub>2</sub> storage in aquifers. *SPE J.* (2005) 10(03), 336-348